Journal of Applied Sciences

ISSN 1812-5654

science alert

ANSInet
an open access publisher
http://ansinet.com

Journal of Applied Sciences 8 (11): 2050-2058, 2008
ISSN 1812-5654

Analysis of Chatter Stability in Facing

S. Kebdani, A. Sahli, O. Rahmani, D. Boutchicha and A. Belarbi
Department of Mechanical Engineering, University of Sciences and Technology,
B.P. 1505 Oran El Menaouer, 31000, Algeria

Abstract: This study attempts to develop a chatter model for predicting chatter stability conditions in hard turning. A linear model is developed by introducing non-uniform load distribution on a tool tip to account for the flank wear effect. Stability analysis based on the root locus method and the harmonic balance method is conducted to determine a critical stability parameter. To validate the model, a series of experiment is carried out to determine the stability limits as well as certain characteristic parameters for facing and straight turning. Chatter in hard turning has the feature that the critical stability limits increase very rapidly when the cutting speed is higher than 13 rev sec^{-1} for all feed directions. The main contributions of the study are threefold. First, chatter-free cutting conditions are predicted and can be used as a guideline for designing tools and machines. Second, the characteristics of chatter in hard turning, which is observed for the first time, helps to broaden our physical understanding of the interactions between the tool and the workpiece in hard turning. Third, experimental stability limits for different flank wear can contribute to lead more reasonable ways to consider the flank wear effect in chatter models of hard turning. Based on these contributions, the proposed linear chatter model will support to improve the productivity in many manufacturing processes. In addition, the chatter experimental data will be useful to develop other chatter models in hard turning.

Key words: Chatter model, predicting, hard turning, workpiece

INTRODUCTION

Chatter is a self-excited mechanical vibration during machining processes. It causes adverse effects such as the poor surface finish of the workpiece, reduced tool life and eventually the loss of productivity (Tewani *et al.*, 1995). The limit of cutting parameters to avoid chatter can be less conservative if chatter stability is predicted in terms of cutting conditions. Therefore the prediction of chatter is one of crucial factors for achieving high productivity in machining operations.

The prevention of chatter is even more important in hard turning than conventional mild turning. Recently hard turning has been actively investigated since it has the potential to replace more costly and less agile grinding processes in finishing hardened materials of HRC 45-70. Considering the surface quality demand in finishing and the relatively brittle property of PCBN inserts, hard turning is more sensitive to the occurrence of chatter. Unfortunately, there have been few theoretical and experimental investigations on chatter associated with hard turning.

Flank wear is an important factor to consider in the modeling of chatter for hard turning. The strong relation between flank wear and cutting force has been reported for hard turning (Wang and Liu, 1999; Chou and Evans, 1999). It was suggested that cutting force increases for larger flank wear in machining hardened steels. As chatter stability is clearly affected by flank wear in mild turning (Fofana *et al.*, 2003; Elbestawi *et al.*, 1991; Chiou and Liang, 1998), flank tool wear is also suggested as one of primary sources of chatter in hard turning (Davies, 1998). In addition, Kishawy and Elbestawi (1999) showed tool wear also affected machined surface quality during hard turning. Therefore, it is necessary to introduce an appropriate method to consider the flank wear effect in the modeling of chatter for hard turning.

One of challenging aspects in the modeling of chatter is that there are infinitely many roots of the characteristic equation on the imaginary axis, which correspond to the critical stability parameter. When the regenerative effect is considered as a main mechanism of chatter, a closed loop characteristic equation has a time delay term, which is a period of one revolution in the machining process. Since the time delay results in infinitely many roots on the imaginary axis, it has been a key issue to determine critical values of the stability parameter among infinitely many roots in stability analysis involving chatter problems. In this study, critical stability parameters have been determined explicitly by drawing root loci in terms of the

Corresponding Author: S. Kebdani, Department of Mechanical Engineering, University of Sciences and Technology, B.P. 1505 Oran El Menaouer, 31000, Algeria

stiffness ratio with the presence of flank wear. Furthermore, the effect of a time delay on chatter stability is also discussed.

In this study, linear chatter modeling procedures for facing operations are described. The characteristic equation with non-uniform load distribution is derived to consider the flank wear effect. Then the root locus method for general worn tools, which explicitly decides the critical stability parameter in stability analysis, is described.

LINEAR MODELING FOR CHATTER IN FACING

In this study, a 1-DOF linear chatter model considering the flank wear effect is developed. It is assumed that the workpiece is rigid and the flexible tool is able to vibrate only in the *x* direction as shown in Fig. 1. The feed direction in facing operations is

$$m\ddot{x}(t) + c\ddot{x}(t) + k_m x(t) = \Delta F_x(t) \tag{1}$$

where, m is the mass of the tool, c is the damping coefficient, k_m is the structural stiffness and $\Delta F_x(t)$ is the amount of variation in the x-component of cutting force.

The variation of cutting force ΔF_x in Eq. 1 is caused by the variation of uncut chip thickness during consecutive turns in the machining process, as shown in Fig. 2.

Any irregular motion of a tool makes an undulated surface during machining process and it leads the deviation in uncut chip thickness from a nominal value at the next revolution, which results in the variation of cutting force. This phenomenon is called the regenerative effect, which induces ΔF_x for a sharp tool as the following:

$$\Delta F_x(t) = k_c[x(t) - x(t - T_p)] \tag{2}$$

where, k_c is cutting stiffness, x(t) and $x(t-T_p)$ are deviations from the equilibrium position of the tool edge at the current turn and the previous turn, respectively and T_p is the period of a turn.

In the present study, non-uniform load distribution on the flank wear area is introduced to consider the flank wear effect in the chatter model. Two different approaches have been used mainly to include the effect of flank wear (Waldorf *et al*., 1998). Wu (1988) suggested a method to represent the flank wear effect by employing contact force, which is proportional to the displaced volume of the workpiece beneath the tool. Based on the contact force model, Elbestawi *et al*. (1991) predicted an increased

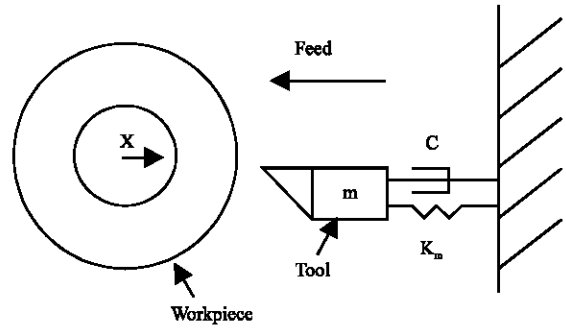

Fig. 1: Schematic diagram of the tool-workpiece system

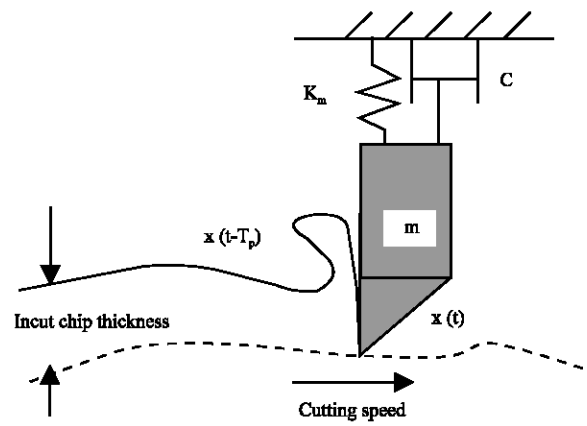

Fig. 2: Schematic diagram of the regenerative effect in facing

chatter-free region in numerical simulations for larger tool flank wear. The same tendency that tool flank wear stabilized chatter vibration was experimentally verified in mild turning by Chiou and Liang (1998) and Clancy and Shin (2002). However, it is difficult to extend the contact force model to hard materials since the uncertainty in estimating displaced volume increases. Another way to consider the flank wear effect is based on the slip-line model, which was originally proposed by Challen and Oxley (1979). Cutting force including ploughing force due to the existence of flank was predicted by this method (Black *et al*., 1993). Considering the slip-line field and the presence of plastic flow of the workpiece under the tool flank (Kobayashi and Thomsen, 1960; Thomsen *et al*., 1962; Smithey *et al*., 2001). Waldorf (1996) introduced nonuniform stress distribution along the flank wear area to estimate force on the worn area.

Furthermore, Stepan (1998) suggested a chatter model with non-uniform load distribution on the active face between the workpiece and the tool. However, a chatter model with non-uniform load distribution on the flank wear area has not been attempted. In this study, the

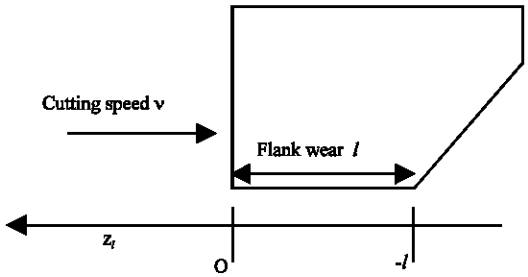

Fig. 3: Schematic diagram of the tool tip with the flank wear length of l and local coordinate z_l along flank wear

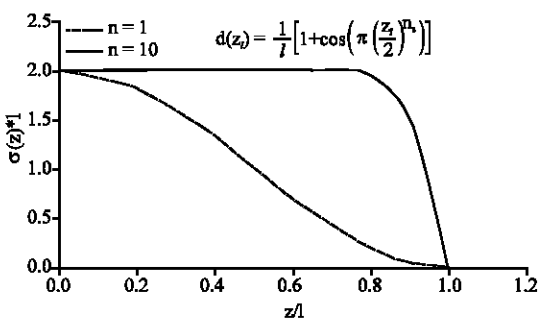

Fig. 4: Non-uniform load distribution along flank wear

method to integrate non-uniform load distribution on flank wear has been employed for considering the flank wear effect to avoid the uncertainty in estimating the displaced volume of hard materials.

In the present study, non-uniform load distribution $\sigma(z_l)$ is assumed in the local coordinate z_l along flank wear as the following (Fig. 3):

$$\sigma(z_l) = \frac{1}{l}\left[1+\cos\left(\pi\frac{z_l}{l}\right)^{ns}\right], \quad z_l \varepsilon [-1,0] \tag{3}$$

where, l is the length of flank wear. The exponent ns is to determine how much plastic deformation occurs and is assumed to be inversely proportional to the flank wear length l as the following:

$$n_s = \frac{\alpha}{l} \tag{4}$$

where, α is a positive constant. As shown in Fig. 4, this load distribution has the maximum value at the beginning of flank wear and becomes zero at the end of flank wear. This form of load distribution has ability to reflect the effects of the flank wear length as well as the degree of plastic deformation of the workpiece under flank wear. As a result, the effect of plastic deformation and flank wear on chatter stability can be examined through this load distribution.

Let us introduce h which is the duration to pass the interface of length l between the tool and the workpiece at the speed of v:

$$h = \frac{l}{v} \tag{5}$$

Converting non-uniform load distribution of Eq. 2-5 into the form in local time θ yields

$$\sigma(\theta) = \frac{1}{h}\left[1+\cos\left(\pi\frac{\theta}{h}\right)^{ns}\right], \quad \theta\varepsilon[-h,0] \tag{6}$$

When load distributions on a finite length of the tool as well as the regenerative effect are considered, ΔFx(t) in Eq. 2 becomes as the following:

$$\Delta F_x(t) = k_c\int_{-T_{p-h}}^{-T_p}\sigma(T_p+\theta)x(t+\theta)d\theta - kc\int_{-h}^{0}\sigma(\theta)x(t+\theta)d\theta \tag{7}$$

where, kc is the cutting stiffness and Tp is the period of the workpiece. Substituting the cutting force variation in Eq. 7 into the differential Eq. 1 and dividing the both sides by m yields

$$\begin{aligned} &m\ddot{x}(t) + 2\omega n\varsigma x(t) + \omega_n^2 x(t) \\ &= \frac{k_c}{k_m}\omega_n^2\int_{-T_{p-h}}^{-T_p}\sigma(T_p+\theta)x(t+\theta) \\ &d\theta - \frac{k_c}{k_m}\omega_n^2\int_{-h}^{0}\sigma(\theta)x(t+\theta)d\theta \end{aligned} \tag{8}$$

where, $\omega_n = (km/m)^{1/2}$ is the natural frequency of the system and $\varsigma = c/(2m\ \omega_n)$ is the damping ratio of the system. The regenerative effect which reflects the position difference between the previous turn and the present turn yields two terms on the right side of Eq. 8 and the flank wear effect is considered by integrating load distribution $\sigma(\theta)$ for each term. Performing the Laplace transform of Eq. 8 with zero initial conditions and rearranging resulting terms yield the characteristic equation for a worn tool with non-uniform load distribution:

$$s_2 + 2\varsigma\omega_n s + \omega_n^2 + \frac{k_c}{k_m}\omega_n^2\int_{-h}^{0}\sigma(\theta)e^{s\theta}d\theta(1-e^{-sTp}) = 0 \tag{9}$$

When the value of ns is 1 and *l* is negligibly small, load distribution $\sigma(\theta)$ becomes the Dirac delta function corresponding to the load distribution of an ideal sharp tool. The Dirac delta function $\delta(\theta)$ has the following filtering property. Suppose $\gamma > 0$ and let f be integrable on [0, ∝[and continuous at γ. Then

$$\int_0^{\infty} f(x)\delta(x-y)dx = f(\gamma) \tag{10}$$

Therefore, the value of integral in Eq. 9 becomes unity so that

$$\int_{-h}^{0} \sigma(\theta)e^{s\theta}d\theta = \int_{-h}^{\infty} \delta(\theta)e^{s\theta}d\theta = 1 \tag{11}$$

The characteristic equation for a sharp tool is derived from Eq. 9 and 11 and is shown as

$$s_2 + 2\varsigma\omega_n s + \omega_n^2 + \frac{k_c}{k_m}\omega_n^2(1-e^{-sTp}) = 0 \tag{12}$$

STABILITY ANALYSIS FOR WORN TOOLS

Determination of the critical stability parameter: The system is stable if all of roots of the closed loop characteristic equation have negative real values. If any of roots have zero real values, the rest having negative real values, then this represents the critical condition of stability. Because the closed loop characteristic equation with a time delay has infinitely many roots on the imaginary axis, it has been a crucial issue in stability analysis to derive the critical parameter among infinitely many roots which determines the stability of the system. In chatter stability problems that also include a time delay, the stiffness ratio, kc/km is a commonly used parameter when stability is decided for a given time delay.

There have been many attempts to obtain the critical kc/km resolving the complexity in stability analyses caused by the transcendental nature of the characteristic equation for chatter problems. For example, Tlusty and Polacek (1963) and Merritt (1965) developed fundamental chatter theories that determined the chatter frequency and the stiffness ratio for a time delay by simultaneously solving two equations at $s = j\omega$, which were derived from the characteristic equation. Nyquist stability criterion was employed by Minis *et al.* (1990) as an alternative approach to derive the critical stability parameter. In addition, the root locus method determined the critical stiffness by finding the first pair of roots on the imaginary axis while the others remained in the stable left hand side of the complex plane (Olgac and Hosek, 1998). The Routh-Hurwitz stability criterion also can be used for time-delayed systems after transforming a transcendental equation to a polynomial equation (Rekasius, 1980).

In the present study, critical parameters for chatter stability are explicitly determined by drawing root loci in terms of the stiffness ratio. Even though the methodology is not new, this is the first attempt to expand the root locus method in stability analyses to more general worn tool cases. The condition of root loci to have the minimum stiffness ratio as the critical parameter is derived after finding poles and zeros and categorizing branches in the root locus plot.

First of all, locations of roots with zero and infinite values of the stiffness ratio, which correspond to poles and zeros of the open loop system, are found analytically.

There are an infinite number of poles at $s = -\infty \pm j\,2n\pi/Tp$ (n = 0, 1, 2,...) as well as two finite poles at

$$s = -\varsigma\omega_n \pm \sqrt{\varsigma^2\omega_n^2 - \omega_n^2}.$$

The closed loop system also has an infinite number of zeros on the imaginary axis at $s = \pm j2n\pi/Tp$ (n = 0, 1, 2,...). Therefore, the gap between branches decreases as the amount of time delay increases.

In addition to locations of poles and zeros of the open loop system, it is necessary to know if any root of the closed loop characteristic equation has a positive real part, which induces chatter for given cutting conditions. In this study, whether roots of the closed loop characteristic equation have a positive sign is determined analytically According to the results, there are two kinds of branches in the root locus diagram following these criteria:

- One always remains in the left-hand side of the s-plane and ends at one of zeros on the imaginary axis,

$$\text{if } \int_{-h}^{0} \sigma(\theta)\cos\left(\frac{2n\pi\theta}{T_p}\right)d\theta > 0 \quad \text{for } \omega_n > \frac{2n\pi}{T_p} \tag{13a}$$

$$\text{if } \int_{-h}^{0} \sigma(\theta)\cos\left(\frac{2n\pi\theta}{T_p}\right)d\theta < 0 \quad \text{for } \omega_n < \frac{2n\pi}{T_p} \tag{13b}$$

- The other crosses the imaginary axis only once from the left-hand side to the right-hand side of the s-plane and ends at one of zeros on the imaginary axis,

$$\text{if } \int_{-h}^{0} \sigma(\theta)\cos\left(\frac{2n\pi\theta}{T_p}\right)d\theta < 0 \quad \text{for } \omega_n > \frac{2n\pi}{T_p} \tag{14a}$$

$$\text{if } \int_{-h}^{0} \sigma(\theta)\cos\left(\frac{2n\pi\theta}{T_p}\right)d\theta > 0 \quad \text{for } \omega_n < \frac{2n\pi}{T_p} \tag{14b}$$

Because roots have positive real parts, the second type of branches is related to the instability of the closed loop system. Whether a branch has an unstable root or not depends on the value of the zero of the branch as well as the amount of a time delay and load distribution. Since in this study values of

$$\int_{-h}^{0} \sigma(\theta)\cos\left(\frac{2n\pi\theta}{T_p}\right)$$

are always positive for a given load distribution, the natural frequency, the amount of a time delay and the order of a branch determine if it has unstable roots. If $\omega n > 2n\pi/Tp$, n = 0, 1, 2,..., then branches remain in the stable left hand side of the s-plane. On the contrary, if $\omega n < 2n\pi/Tp$, n = 0, 1, 2,..., then branches approach to zeros on the imaginary axis with positive real parts.

When a fair of branch reach the imaginary axis in the root locus plot, the other branches being in the left hand side of the s-plane, the value of the stiffness ratio at the imaginary axis corresponds to the instability of the system. If branches crossing the imaginary axis never return to the left-hand side of the s-plane and it is possible to find the minimum value of the stiffness ratio on the imaginary axis, then the minimum stiffness ratio is the critical parameter to determine the stability of the closed loop system. In the present study, branches remain in the right hand side of the s-plane as the stiffness ratio is increased to infinite once crossing the imaginary axis. Therefore, the critical stiffness ratio is the minimum value of the stiffness ratio among infinitely many branch crossings on the imaginary axis. Procedures to obtain the minimum kc/km in the root locus of the closed loop system are summarized as follows:

- For a given value of a time delay, determine the value of branch identifier n, which satisfies $\omega n < 2n\pi/T p$.
- The nth branch of the root locus plot is drawn as the gain kc/km changes from zero to infinity.
- The value of kc/km on the imaginary axis is calculated by an interpolation method.
- The above procedures are repeated for increasing *n* until the minimum value of kc/km on the imaginary axis is found.

For instance, the minimum kc/km is found in the root locus of the closed loop system when Tp = 0.1 sec, $\omega n = 111$ Hz and $\varsigma = 0.054$. The condition of $\omega n < 2n\pi/Tp$ is satisfied when n is larger or equal to 12. The value of the stiffness ratio on the imaginary axis is calculated for an increased value of n starting from 12. In this case, the branch of n =12 has the minimum value of the stiffness ratio on the imaginary axis according to numerical calculations. The frequency corresponding to the minimum stiffness ratio is the chatter frequency and it is larger than the natural frequency of the system.

Time delay effect on chatter stability: The effect of a time delay Tp on the stability has been found for a worn tool. If the real part of (ds/dTp) at s = jω is positive, then it means the root crosses the imaginary axis from the left side to the right side parallel to the real axis. Therefore, an increase in the time delay makes the system unstable with the positive real part of (ds/dTp) at s = jω. For a worn tool with the flank wear length of *l* and load distribution σ(θ), the real part of (ds/dTp) at s = jω has the sign in accordance with:

$$\operatorname{sgn}\left[\operatorname{Re}\left(\frac{ds}{dTp}\bigg|_{z=j\omega}\right)\right] = \operatorname{sgn}\left\{\frac{1}{\omega}\left[\begin{array}{l}\left(\frac{k_c}{k_m}\omega_n^2\right)^2(I_{tc}I_s - I_cI_{ts}) + (2\xi\omega_n + \frac{k_c}{k_m}\omega_n^2 I_{tc}) \\ (2\varsigma\omega_n + \frac{k_c}{k_m}\omega_n^2 I_s) - (2w + \frac{k_c}{k_m}\omega_n^2 I_{ts}) \\ (-\omega^2 + \omega_n^2 + \frac{k_c}{k_m}\omega_n^2 I_c)\end{array}\right]\right\} \tag{15}$$

$$I_c = \int_{-h}^{0}\sigma(\theta)\cos\theta d\theta \qquad I_{tc} = \int_{-h}^{0}\sigma(\theta)\cos\theta d\theta \tag{16a}$$

$$I_s = \int_{-h}^{0}\sigma(\theta)\sin\theta d\theta \qquad I_{ts} = \int_{-h}^{0}\sigma(\theta)\sin\theta d\theta \tag{16b}$$

Therefore, if the sign of Eq. 15 is positive, the high cutting speed region has more aggressive cutting conditions remaining chatter-free environment than the low cutting speed region since the time delay is the inverse of cutting speed.

Stability analysis for sharp tools: A stability analysis for a sharp tool can be derived as a special case of a stability analysis for a worn tool. When *ns* is equal to 1 and flank wear length *l* is negligibly small in non-uniform load distribution σ(θ), load distribution becomes the Dirac delta function δ(θ). This is the load distribution corresponding to chatter stability models for a sharp tool, which have been studied for several decades (Merritt, 1965; Minis *et al*., 1990; Olgac and Hosek, 1996). Characteristics of the root locus and the time delay effect on stability for a sharp tool can be obtained by

substituting $\delta(\theta)$ into $\sigma(\theta)$ of above results. It turned out that the locations of poles and zeros for a sharp tool case are the same as those for a worn tool. In addition, branches in the root locus plot of a sharp tool have positive real parts for $\omega_n < 2n\pi/T_p$ since the integrals in Eq. 13 have the unity value.

Furthermore, if

$$\omega^2 - \omega_n(1+\frac{k_c}{k_m}) + 2\varsigma^2\omega_n^2 > 0$$

the system becomes unstable as the time delay T is increased.

PREDICTIONS OF CHATTER STABILITY IN FACING

Theoretical predictions of chatter stability are attempted with the linear modeling of chatter in facing of hardened materials, which considers the flank wear effect through non-uniform load distribution on a worn area of tools. In order to achieve more realistic predictions, the unique features of hard turning such as the cutting speed effect involved with high temperature should be considered in the predicting processes. In the present study, the effect of the cutting speed is considered through measuring the cutting stiffness at different cutting speed values.

After conducting a series of experiments to measure characteristic parameters required in the proposed modeling of chatter, critical stiffness ratios are predicted for a given range of cutting speed. In addition, a converting relation between the stiffness ratio and the width of cut is obtained reflecting the effect of cutting speed. The flank wear effect is examined and discussed based on resultant stability charts for different flank wear values. A tangential stability line is proposed for more practical use of stability charts especially in the low cutting speed range.

Measurements of characteristic parameters: Characteristic parameters of the tool system are determined by a series of experimental measurements. Since it is assumed that the tool system is the only flexible component in the model, the natural frequency, the damping ratio, the structural stiffness and the cutting stiffness of the tool system should be measured for the theoretical prediction of chatter stability in machining processes. Furthermore, the relation between the stiffness ratio and the width of cut is obtained to plot the stability chart in terms of the width of cut instead of the stiffness ratio. Results of characteristic parameter measurements are summarized in Table 1.

Table 1: Characteristic parameters of the tool system

Workpiece	Hollow bar Length = 76.2 mm Outer diameter = 41.2 mm Inner diameter = 26.9 mm
Natural frequency	111 Hz
Damping ratio	0.054
Structural stiffness	5600 N/mm
Cutting stiffness	985 N/mm(at the width of cut = 0.508 mm and the cutting speed = 14 rps)

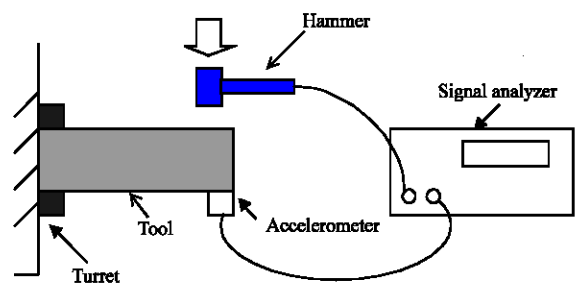

Fig. 5: Schematic diagram of impact testing for measuring the natural frequency ω_n and the damping ratio ς

The natural frequency and the damping ratio of the tool system are determined by impact testing. Attaching an accelerometer on a side of the tool, frequency responses are obtained by applying an impact with a hammer at the opposite side of the tool system as shown in Fig. 5. The peak at the lowest frequency is chosen as the natural frequency of the tool system in the averaged frequency response. The damping ratio is decided by observing how fast the magnitude of the peak of the natural frequency diminished along with frequency variation. The main processes to obtain the damping ratio of the tool system are finding two points corresponding to 0.707 times the maximum magnitude of the peak and then calculating frequency difference between these two points. As a result of impact testing, it turned out that the natural frequency of the tool system is 111 Hz and the damping ratio is 0.054.

The structural stiffness is obtained by simultaneous measurements of displacement and static force applied at the end of the workpiece through the tool. The workpiece is 76.2 mm long and assumed as a rigid body. The displacement of the tool system relative to the hollow bar is measured by a dial gage and static force exerted on the tool tip is measured by a dynamometer as shown in Fig. 6. The structural stiffness of the tool system is determined as 5320 N/mm.

The cutting stiffness is found by measuring thrust force for given cutting conditions in the cutting operation. As seen in Fig. 7, the dynamometer connected to the tool system of the machine measured thrust force as the cutting process is performed at the end of the system of

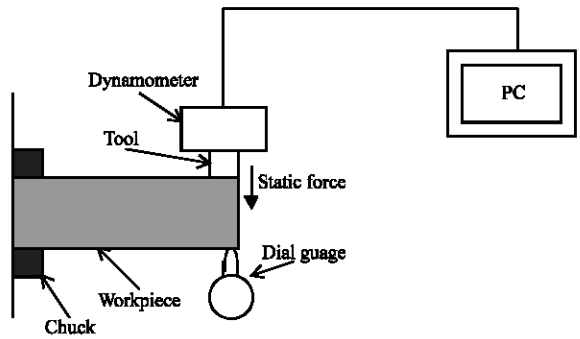

Fig. 6: Schematic diagram of the experimental setup for measuring the structural stiffness k_m

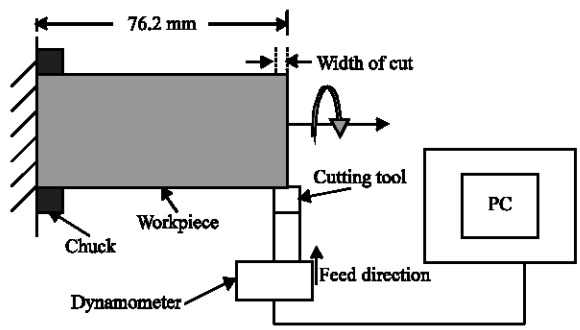

Fig. 7: Schematic diagram of the experimental setup for measuring the cutting stiffness k_c in facing

76.2 mm long work piece. In the present study, thrust force is assumed to be linearly proportional to uncut chip thickness or the feed rate and the proportionality constant is the cutting stiffness. Thrust force is measured for three different values of the width of cut in the range of the feed rate from 0.0127 to 0.0508 mm rev^{-1} and results are shown in Fig. 8. All facing operations are operated with slightly worn tools, which have flank wear in the range from 40 to 60 μm. The slope of the curves corresponding to the cutting stiffness is increased slightly along with an increase of the width of cut. Thrust force measurements as a function of the feed rate for two different values of cutting speed are represented in Fig. 9. Thrust force and the cutting stiffness decrease for higher cutting speed. These tendencies in force measurements are well matched with existing experimental investigations on hard turning (Chou and Evans, 1999). The cutting stiffness is determined as 985 N/mm from those cutting force data when the width of cut is 0.508 mm and the cutting speed is 14 rps.

The relation between the stiffness ratio and the width of cut is obtained from cutting force data of machining of hardened 52100 steels. In this study, the

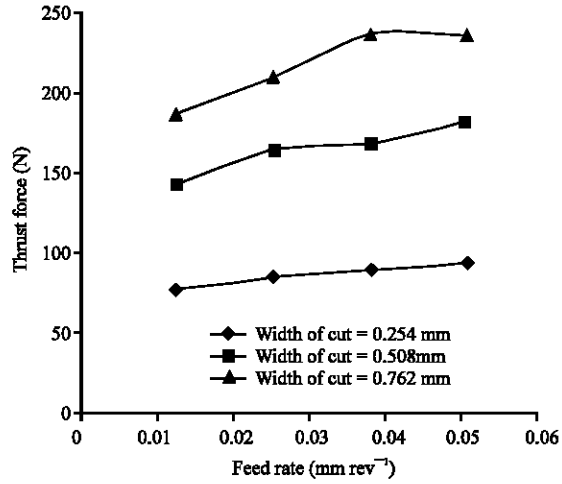

Fig. 8: Thrust force versus the feed rate at the cutting speed of 14 rev sec^{-1}

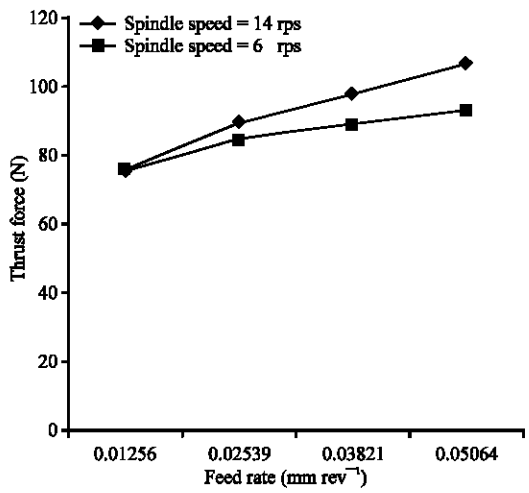

Fig. 9: Thrust force versus the feed rate at the width of cut of 0.254 mm

stability chart is plotted in terms of the width of cut instead of the stiffness ratio since the width of cut is a more practical parameter in machining operations. Chiou and Liang (1998) converted the stiffness ratio to the width of cut by multiplying a constant, which is derived from force measurements. Here, the converting relation is obtained as a function of cutting speed to reflect the dependence of the cutting stiffness on cutting speed, which is clearly shown in Fig. 9. The converting relation is derived as:

$$\text{woc} = (0.031\Omega + 2.6)\left(\frac{k_c}{k_m}\right) + (0.02\Omega - 0.3)$$

where, woc is the width of cut.

Predictions of stability limit in facing: Based on the stability analysis and parameter measurements in previous sections, the stability chart is obtained to predict chatter-free cutting conditions. The minimum stiffness ratio kc/km is obtained in the root locus for a given time delay and the same procedures are repeated for the range of cutting speed. Since the minimum kc/km is the critical stability parameter as shown in the stability analysis, the region above the minimum stiffness ratio is called the unstable region. The region below the minimum stiffness ratio is called the stable region where there is no chatter for a given cutting speed. Values of the width of cut corresponding to minimum stiffness ratios are obtained by means of the converting relation derived from force measurement data. For non-uniform load distribution, the values of flank wear length l are 0.0254, 0.0762 and 0.127 mm and the value of ns are assumed as 0.5.

In order to show the dependency of the flank wear effect on cutting speed, the area of the stable region is calculated for 4 different speed divisions, respectively. As shown in Fig. 10, the total area under the stability line is increased as the length of flank wear is increased and the stabilizing effect is most dominantly appeared in the high-speed range ($12 < \Omega < 15$ rps).

The question of whether a stability line with more conservatism can be used as an alternative to the original stability line for more practical use of the stability chart is now examined. Because a small change in cutting speed causes a large variation in the predicted stability line in the low cutting speed range and the length of flank wear can change during machining processes, it is necessary to apply a conservative prediction for proper machining operations. This stability line is called a tangential stability line and it provides more conservative chatter prediction in the stability chart. As seen in Fig. 11, the tangential stability line shows the same tendency as is shown by the original stability line for different values of flank wear.

Therefore, the tangential stability line can be used as an alternative stability line, reflecting the stabilizing effect due to flank wear. Another conservative stability line can be derived from stability charts for sharp tools. In stability charts for sharp tools, the closed loop system is always stable regardless of the amount of time delay when kc/km is less than $2\varsigma(\varsigma+1)$. This stability line is called an absolute stability line. In addition, the prediction for a sharp tool provides very similar stability limits compared with the stability line for the worn tool with flank wear of 0.0254 mm. Therefore, the flank wear effect can be negligible when the length of flank wear is less than 0.0254 mm.

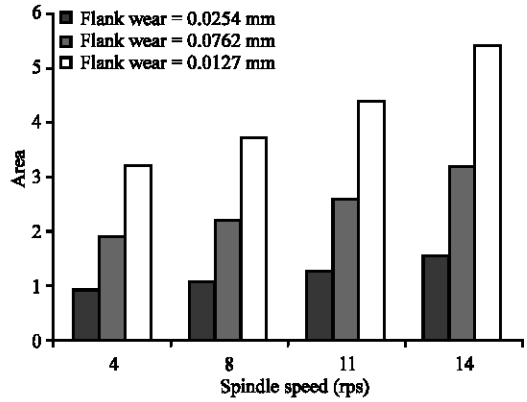

Fig. 10: Area under the stability line for different values of flank wear

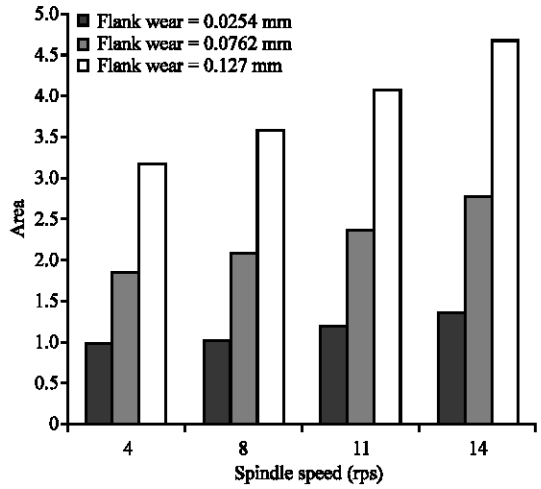

Fig. 11: Area under the tangential stability lines for different values of flank wear

CONCLUSION

A new modeling of chatter for facing has been developed considering the flank wear effect through non-uniform load distribution on flank wear. Having a more realistic load distribution reflecting the change of the flank wear length as well as the degree of the plastic deformation, a stability analysis has been carried out to determine the critical stability parameter for worn tools. The minimum stiffness ratio is the critical stability parameter based on characteristics of branches in the root locus found in stability analysis. It is shown that stability is affected by a time delay, characteristic parameters and the load distribution. Stability charts for sharp tools are obtained as a special case of the present chatter model.

Characteristic parameters of a tool system have been measured for predicting stability limits in facing from the

proposed model. In order to consider the cutting speed effect, the values of the cutting stiffness are measured at two cutting speeds while the range of flank wear is between 40 and 60 μm. Theoretical predictions of stability have been obtained from measured characteristic parameters. The minimum stiffness ratios are obtained for a range of speed with the root locus method and then stability charts in the width of cut are plotted employing the converting relation. The stabilizing effect of flank wear is clearly shown in tangential stability lines as well original stability lines from theoretical predictions. The absolute stability line is derived as the most conservative stability guideline.

REFERENCES

Black, A.J., E.M. Kopalinsky and P.L.B. Oxley, 1993. Asperity deformation models for explaining the mechanisms involved in metallic sliding friction and wear-A review. J. Mech. Eng. Sci., 207 (4): 335-353.

Challen, J.M. and P.L.B. Oxley, 1979. An explanation of the different regimes of friction and wear using asperity deformation models. Wear, 53 (2): 229-243.

Chiou, R.Y. and S.Y. Liang, 1998. Chatter stability of a slender cutting tool in turning with tool wear effect. Int. J. Mach. Tools Manuf., 38 (4): 315-327.

Chou, Y.K. and C.J. Evans, 1999. White layers and thermal modeling of hard turned surfaces. Int. J. Mach. Tools Manuf., 39 (12): 1863-1881.

Clancy, B.E. and Y.C. Shin, 2002. A comprehensive chatter prediction model for face turning operation including tool wear effect. Int. J. Mach. Tools Manuf., 42 (9): 1035-1044.

Davies, M.A., 1998. Dynamic Problems in Hard-Turning, Milling and Grinding. Dynamics and Chaos in Manufacturing Processes, John Wiley and Sons, New York, pp: 57-91.

Elbestawi, M.A., F. Ismali, R.X. Du and B.C. Ullagaddi, 1991. Modeling machining dynamics including damping in the tool-workpiece interface. J. Eng. Ind., 116 (4): 435-439.

Fofana, M.S., K.C. Ee and I.S. Jawahir, 2003. Machining stability in turning operation when cutting with a progressively worn tool insert. Wear, 255 (7-12): 1395-1403.

Kishawy, H.A. and M.A. Elbestawi, 1999. Effects of process parameters on material side flow during hard turning. Int. J. Mach. Tools Manuf., 39 (7): 1017-1030.

Kobayashi, S. and E.G. Thomsen, 1960. The role of friction in metal cutting. J. Eng. Ind. Trans. ASME., 82 (3): 324-332.

Merritt, H.E., 1965. Theory of self-excited machine -tool chatter. J. Eng. Ind. Trans. ASME., 87 (4): 447-454.

Minis, I.E., E.B. Magrab and I.O. Pandelidis, 1990. Improved methods for the prediction of chatter in turning, Part 3: A generalized linear theory. J. Eng. Ind. Trans. ASME., 112 (1): 28-35.

Olgac, N. and M. Hosek, 1998. A new perspective and analysis for regenerative machine tool chatter. Int. J. Mach. Tools Manuf., 38 (7): 783-398.

Rekasius, Z.V., 1980. A stability test for systems with delays. In: Proceedings Joint Automatic Control Conference, Paper No. TP9-A.

Smithey, D.W., S.G. Kapoor and R.E. DeVor, 2001. A new mechanistic model for predicting worn tool cutting forces. Mach. Sci. Technol., 5 (1): 23-42.

Stepan, G., 1998. Delay-Differential Equation Models for Machine Tool Chatter. Dynamics and Chaos in Manufacturing Processes, John Wiley and Sons, New York, pp: 165-191.

Tewani, S.G., K.E. Rouch and B.L. Walcott, 1995. A study of cutting process stability of a boring bar with active dynamic absorber. Int. J. Mach. Tools Manuf., 35 (1): 91-108.

Thomsen, E.G., A.G. MacDonald and S. Kobayashi, 1962. Flank friction studies with carbide tools reveal sublayer plastic flow. J. Eng. Ind. Trans. ASME. Ser. B, 84 (1): 53-62.

Tlusty, J. and M. Polacek, 1963. The stability of the machine tool against self- excited vibration in machining. ASME Production Engineering Research Conference, Pittsburgh.

Waldorf, D.J., 1996. Shearing, ploughing and wear in orthogonal machining. Ph.D Thesis, University of Illinois at Urbana-Champaign.

Waldorf, D.J., R.E. DeVor and S.G. Kappor, 1998. A slip-line field for ploughing during orthogonal cutting. ASME. J. Manuf. Sci. Eng., 120 (4): 693-699.

Wang, J.Y. and C.R. Liu, 1999. The effect of tool flank wear on the hear transfer, thermal damage and cutting mechanics in finish hard turning. Ann. CIRP., 48 (1): 53-58.

Wu, D.W., 1988. Application of a comprehensive dynamic cutting force model to orthogonal wave generating processes. Int. J. Mech. Sci., 30 (8): 581-660.